

Graphic determination of available energy-saving potential in a reservoir pumping application with variable-speed operation

Tero Ahonen  · Santeri Pöyhönen · Joni Siimesjärvi · Jukka Tolvanen

Received: 8 December 2016 / Accepted: 1 July 2018 / Published online: 12 July 2018
© Springer Nature B.V. 2018

Abstract Centrifugal pumps represent a notable share of electricity consumption in motor-driven systems. Many studies have verified the energy-saving potential in these systems with device improvements and by modification of the applied flow control method or characteristics of the surrounding process. The best approach for reaching a more energy-efficient reservoir pumping system has to be determined for each system separately, making the analysis too laborious for a typical system operator. This paper proposes the application of graphic analysis tool for determination of the available energy saving potential in a reservoir pumping application. To realize this object, this paper studies how the available energy-saving potential in a reservoir pumping system is affected by two different variable-speed control schemes and by surrounding process variables, namely the static head variation and friction factor. Based on conducted simulations, generic graphs for determination of the available energy saving potential in the reservoir pumping application are formed, and their applicability is tested with two real-life cases. The produced graphs for available energy-saving potential seem to provide feasible results when compared to the case studies, justifying their use for instance in energy audits. Hence, this paper provides an effective tool for

pumping station operators to assess economic feasibility of a variable-speed operation in their systems. However, further testing is required to see whether the resulted graphs are representing reality in all situations that can be described with static head and its variation.

Keywords Energy audits · Energy efficiency · Pumps · Reservoir pumping application · Variable-speed drives

Introduction

Centrifugal pumps represent a notable share of electricity consumption in motor-driven systems. In addition, energy efficiency improvements in pumping systems directly affect the resulting energy consumption with measurable savings as shown in de Almeida et al. (2003), Kaya et al. (2008), and Lindstedt and Karvinen (2016). Energy efficiency as a term does not only refer to the efficiency of each individual component, but also the system demand for the flow and pressure, applied flow control method and surrounding process parameters, which set the theoretical minimum level for the pumping system energy consumption as introduced in Hovstadius (2005).

Reservoir pumping applications are a typical example of operating centrifugal pumps according to the present and forecasted demand. A repeated filling or draining of a reservoir is for instance required in wastewater transportation systems, where wastewater is transferred from a municipality area to a wastewater

T. Ahonen (✉) · S. Pöyhönen
School of Energy Systems, Lappeenranta University of
Technology, P.O. Box 20, FI-53851 Lappeenranta, Finland
e-mail: tero.ahonen@lut.fi

J. Siimesjärvi · J. Tolvanen
ABB Drives Service, P.O. Box 184, FI-00381 Helsinki, Finland

treatment plant (see Nesbitt 2006 for further description). In such systems, applying a variable-speed operation for the pumps allows reservoir drainage with the minimum energy consumption, which has been a topic of discussion in several studies. In dos Santos and Selegim (2005), the operation of a selection of different reservoir pumping systems was simulated to demonstrate the energy-saving potential of a variable-speed pump control. Zhang et al. (2012) have proposed a model for the optimal sizing and operation of multi-level pumping systems, which also aims to take into account varying energy prices through load shifting. In Ahonen et al. (2015), methods for optimizing the energy efficiency of a reservoir pumping process and for the sensorless identification of the pumping process characteristics are presented. Furthermore, Lindstedt and Karvinen (2016) present an energy-efficient control scheme for systems combined with time limits for the emptying or filling of reservoirs. A review of research on improving the energy efficiency of pumping systems in general is presented in Shankar et al. (2016).

Notable share of existing reservoir pumping systems are driven with the on/off control scheme and at a fixed speed dictated by the induction motor characteristics (e.g., around 1460 rpm). Since pumps are often oversized for the sake of “just to be on the safe side,” they are mostly driven at non-optimal rotational speed leading to increased specific energy consumption and wasted resources; Ahonen et al. (2015) have exemplified how the specific energy consumption in Wh/m^3 is affected by the rotational speed and process static head H_{st} in a municipal wastewater station (see also Hovstadius 1999). Also in terms of time, variable-speed pumps may allow operation at a lowered rotational speed and with increased duration of the drainage event, since the share of drainage event may just be a fraction of the total operating time.

In such cases, retrofitting a fixed-speed pumping system with a variable-speed drive (VSD) and finding the best rotational speed for the pumping application can lead to large savings in terms of energy costs as verified by Barnes (2014) and Lindstedt and Karvinen (2016). To this end, estimation of the available energy-saving potential should be possible for the end-user without extensive calculations or knowledge on the available control schemes for pumping systems. Often just the main parameters of the pump (such as the nominal and

maximum operating values) and application (such as the process static head and desired reservoir level variation) are known, so the estimation should be possible just with this information. Also, the possible effect of existing energy efficiency-based control schemes within the VSD should be covered in the analysis, so the end-user could easily determine the actual benefit of applying such control scheme. With these needs in mind, the end-user could greatly benefit from a graphic analysis tool, which uses the readily available information about the pump and the system as adjustable parameters to determine the energy-saving potential of a fixed-speed-operated reservoir pump system without significant effort. With this analysis approach introduced later in the paper, the analysis of energy-saving potential becomes more intuitive when compared to the sole use of equations, which is the commonly described approach for analyses (see for instance Pump Systems Matter and Hydraulic Institute 2008).

The main objective of this paper is to study the available energy-saving potential in a generic reservoir pumping application as a function of system parameters such as relative static head, when a fixed-speed pump is retrofitted with a VSD having an energy efficiency-based control scheme, which fixes both the effect of over-dimensioning and altering static head during the pumping task. The study is based on simulating a typical centrifugal pump operation with different process parameters. Generic graphs for the available energy-saving potential in the reservoir pumping application are then created and proposed as a tool for energy audits, which can be considered as the main novelty of this paper. Applicability of the calculus is finally tested with two wastewater station cases.

After this introductory section, this paper divides into five main sections. The “Reservoir pumping system operated with a variable-speed drive” section introduces the applied system variables and the available VSD-based control schemes for reservoir pumping systems. The “Modelling of pumping system operation with different process parameters” section introduces a mathematical model for pumps and a calculation method to gather generic data for graphs. Following to this, the “Results” section illustrates the acquired simulation results, and the “Evaluation of pilot cases” section studies their applicability with two example cases. Finally, the main conclusions of this research work are provided in the “Conclusion” section.

Reservoir pumping system operated with a variable-speed drive

In reservoir pumping applications, fluid is pumped from a reservoir to another, for instance when the allowed fluid level in the supply reservoir is exceeded. In Fig. 1, this kind of reservoir drainage application is illustrated; here, a constant fluid volume V (m^3) is repetitively transferred from supply to the destination reservoir by a pumping system, if there is no notable variation in the inflow to the supply reservoir during the drainage event (Flygt 2015; Lindstedt and Karvinen 2016). As a result of the pumping task, a certain amount of energy E (kWh) is consumed, which allows quantification of the pumping system energy efficiency with the specific energy consumption E_s (kWh/m^3) that is also the relation of power consumption P (kW) and flow rate Q (e.g., in m^3/h):

$$E_s = \frac{E}{V} = \frac{\int P dt}{\int Q dt}. \quad (1)$$

As the pumping lowers the fluid level in the supply reservoir when fluid is transferred to the destination reservoir, the process static head H_{st} (m) increases during the drainage task from $H_{st,s}$ to $H_{st,e}$. This increase in the static head can be estimated with

$$\Delta H_{st} = \frac{V}{A}, \quad (2)$$

when the supply reservoir has a constant floor area A (m^2), and the total volume V (m^3) of the produced flow is known. Even if the reservoir floor area and process static head are affected by the fluid level in both

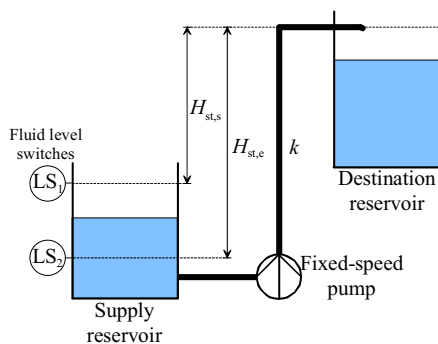


Fig. 1 Scheme of a two-reservoir process. The pump starts to discharge the fluid from the supply reservoir to the destination reservoir when the fluid level reaches LS_1 . The pumping stops when the fluid level reaches LS_2

reservoirs, they can be separately taken into account with the differential equations given in (Lindstedt and Karvinen 2015).

The resulting increase in the process static head affects the instantaneous system E_s and increases the E_s -based optimum rotational speed n_{opt} (rpm) for the pumping system (Ahonen et al. 2015). Since the produced flow rate Q (m^3/s) is not adjusted with control valves during normal operation, the friction loss factor k (s^2/m^5) can be assumed to remain constant. These assumptions result in the following surrounding process characteristics for head:

$$H_{\text{process}}(Q) = H_{st} + k \cdot Q^2 \quad (3)$$

$$\Delta H_{st} = H_{st,e} - H_{st,s}, \quad (4)$$

where H_{process} is the total head loss of the system, H_{st} is always between $H_{st,s}$ and $H_{st,e}$, and the range of this variation is denoted with ΔH_{st} .

The ratio of process static head and its variation during the reservoir drainage are major factors affecting the available energy-saving potential with the variable-speed operation. To make these process variables non-dimensional, and hence generally applicable, they are scaled with the maximum head H_{max} (m) that the pump is able to produce at zero flow rate at its nominal rotational speed n_n (rpm). The reason for using this scaling parameter instead of H_{process} is the object of studying the effect of k on the available energy-saving potential with the variable-speed operation in the “[Effect of surrounding process variables on the available saving potential](#)” section.

VSD-based flow control schemes

When a reservoir pumping system is equipped with a variable-speed drive, the pump can be operated at a desired rotational speed. In the case of typical reservoir drainage application, a variable-speed drive allows energy-efficient system operation for instance at:

- 1) a certain constant rotational speed;
- 2) the optimum rotational speed n_{opt} related to the instantaneous process state (i.e., present H_{st});
- 3) a certain constant flow rate.

The operation at a certain constant rotational speed is easy to implement with several means to find the best reference value: one of the published methods is based on monitoring the energy consumption of each reservoir drainage event and selection of either a lower or higher constant rotational speed for the next drainage event based on the energy consumption of two previous drainage events (see Middleton 2014; Xylem 2013). This method is easy to realize without additional measurements, as it relies on the internal power estimation of VSD.

For systems with changing H_{st} , operation at a constant rotational speed cannot provide the smallest possible energy consumption per emptied reservoir. Thus, the pumping system should be driven at its optimum rotational speed based on the instantaneous process parameters. This control scheme is commonly realized with an external flow rate measurement that is compared to the power consumption information available from a VSD for the instantaneous control of the rotational speed (Kallesøe et al. 2011). Also, soft-sensor-based implementations of this control scheme have been proposed in literature (Ahonen et al. 2015; Tamminen et al. 2013). A control scheme is presented in Ahonen et al. (2015), where the increase in the static head and related optimum rotational speed during the reservoir drainage is compensated with the use of linear rotational speed profile, since it closely correlates with E_s -based optimum rotational speeds. So far, optimization schemes based on instantaneous E_s have not been provided in commercial VSDs.

If the time criterion t has to be considered in the variable-speed operation, pump operation at a constant flow rate

$$Q = \frac{V}{t} \quad (5)$$

provides another simple control scheme for the VSD. As with the E_s -based optimum rotational speed scheme, information on the flow rate can be attained with a separate measurement or by using soft-sensor-based estimation methods. This control method has been evaluated in Lindstedt and Karvinen (2016) where it is shown to be nearly as energy efficient as operating the pump with a linear rotational speed profile. This is caused by the fact that maintaining a constant flow rate during the drainage event will require a continuous increase of the pump rotational speed, making it similar with the linear rotational speed profile introduced above.

Therefore, only control methods 1 and 2 are further studied in this paper.

Modelling of pumping system operation with different process parameters

The calculation of available energy saving potential in a reservoir pumping application requires mathematical models for the pump, the surrounding process and the VSD control schemes. In order to have generic results, the models should also be as generic as possible. Therefore, models introduced in this section are selected so that they can be adjusted with nominal values of the pumping system.

Models for the pump operation

Pump operation can be modeled with polynomial equations that can be easily adjusted to any radial-flow centrifugal pump with knowledge on their main performance values. Schützhold et al. (2013) have provided the following model for pump flow rate Q_n (m^3/s) vs. head H_n (m) characteristic curve at a certain fixed rotational speed n_n (rpm):

$$H_n(Q_n) = H_{\max,n} - (H_{\max,n} - H_{\text{BEP},n}) \cdot \left(\frac{Q_n}{Q_{\text{BEP},n}} \right)^2, \quad (6)$$

where $H_{\max,n}$ is the maximum head produced by the pump at zero flow rate, and $Q_{\text{BEP},n}$ together with $H_{\text{BEP},n}$ indicates the best efficiency point of the pump at the rotational speed n_n . As this polynomial equation provides a generic model for the pump with four easily identifiable parameters ($H_{\max,n}$, $H_{\text{BEP},n}$, and $Q_{\text{BEP},n}$, when the pump is operated at n_n), and it provides similar results as the pump model introduced by Bene (2013), it will be used as the base model for pump operation. Alternatively, the pump model can be constructed with Euler equations, leading to the following second-order polynomial representation of pump head as a function of flow rate and present rotational speed n (rpm):

$$H(Q, n) = a_{h2} \cdot Q^2 + a_{h1} \cdot Q \cdot n + a_{h0} \cdot n^2, \quad (7)$$

where the pump characteristics at n_n are described with polynomial terms a_{h2} , a_{h1} , and a_{h0} (Kallesøe 2005).

When the pump is operated with a VSD, the effect of the present rotational speed n on the pump operation modeled with (6) can be estimated with affinity laws

$$Q(n) = \frac{n}{n_n} \cdot Q_n \quad (8)$$

$$H(n) = \left(\frac{n}{n_n}\right)^2 \cdot H_n \quad (9)$$

$$P(n) = \left(\frac{n}{n_n}\right)^3 \cdot P_n, \quad (10)$$

where subscript n refers to pump quantities at the original rotational speed n_n , at which the model input parameters ($H_{\max,n}$, $H_{\text{BEP},n}$, and $Q_{\text{BEP},n}$) were provided. By combining affinity laws (8) and (9) with (6), the resulting pump model in the QH plane becomes

$$H(Q, n) = \left(\frac{n}{n_n}\right)^2 \cdot H_{\max,n} - \left(\frac{n}{n_n}\right)^2 \cdot (H_{\max,n} - H_{\text{BEP},n}) \cdot \left(\frac{\frac{n_n}{n} \cdot Q}{Q_{\text{BEP},n}}\right)^2. \quad (11)$$

When the pump is operated in a given process, the resulting pump operating points (i.e., Q and H) can be calculated by finding the intersection of (3) and (11) for each time instance of the reservoir drainage. Based on this information, the required power consumption of the pump P (kW) can be calculated for each time instance with

$$P(Q, H) = \frac{\rho \cdot g \cdot Q \cdot H}{\eta(Q)}, \quad (12)$$

where ρ is the fluid density (e.g., 998 kg/m³ for water at 20 °C), g is the acceleration due to gravity (ca. 9.81 m/s²), and η is the pump efficiency that can be approximated for instance with the following model given by Schützhold (2013):

$$\eta_n(Q_n) = \eta_{\text{BEP},n} \cdot \left(\frac{2 \cdot Q_n}{Q_{\text{BEP},n}} - \frac{Q_n^2}{Q_{\text{BEP},n}^2} \right). \quad (13)$$

Often, the pump efficiency is considered to be independent from the instantaneous rotational speed (as in (10)). However, this assumption does not anymore hold true with over $\pm 20\%$ change in the pump rotational speed from its nominal value (Gülich 2003), and therefore, the pump efficiency should be corrected to the instantaneous rotational speed. Gülich (2003) and

Sârbu and Borza (1998) suggest the following equation for centrifugal pumps operated at reduced rotational speeds (i.e., $n < n_n$):

$$\eta(n) = 1 - (1 - \eta_n) \cdot \left(\frac{n_n}{n}\right)^{0.1}. \quad (14)$$

When (13) is inserted to (14) with the consideration of (8), the pump efficiency can be modeled for present flow rate and rotational speed with

$$\eta(Q, n) = 1 - \left(1 - \eta_{\text{BEP},n} \cdot \left(\frac{2 \cdot \frac{n_n}{n} \cdot Q}{Q_{\text{BEP},n}} - \frac{\left(\frac{n_n}{n} \cdot Q\right)^2}{Q_{\text{BEP},n}^2} \right) \right) \cdot \left(\frac{n_n}{n}\right)^{0.1}. \quad (15)$$

Simulation of studied control schemes

The models introduced above allow the simulation of VSD-based control schemes in the Matlab environment. Simulations are based on repeated calculation of the pump operating point at a desired rotational speed in the known process conditions by using (3), (11), and (15). By using (12), the pump power consumption at the current time instance is calculated. The resulting effect of the pump operation on the process static head is solved with (2), and eventually the results for the present time instance are stored to a csv file. This script is repeated until the fluid level in the reservoir (i.e., the process H_{st}) reaches the level LS_2 , corresponding to $H_{\text{st},e}$. At this point, the resulting energy consumption per emptied reservoir (E/V as indicated in (1)) is calculated with the use of trapezoidal integration for the stored power consumption and flow rate values.

This simulation approach was applied to both control schemes. For the best constant speed operation, the simulation was started by determining rotational speed range in which n_{opt} is located during the drainage event. As the best constant speed is somewhere between extreme values $n_{\text{opt},s}$ and $n_{\text{opt},e}$, corresponding to $H_{\text{st},s}$ and $H_{\text{st},e}$, it was found by repeating the simulation script with different rotational speeds from $n_{\text{opt},s}$ to $n_{\text{opt},e}$, and by monitoring the resulting energy consumption per emptied reservoir.

The linear speed profile was determined in a corresponding manner, starting with the determination of $n_{\text{opt},s}$ and $n_{\text{opt},e}$. Following to this, the slope K for the speed profile can be calculated with extreme values

$$K = \frac{n_{\text{opt,e}} - n_{\text{opt,s}}}{H_{\text{st,e}} - H_{\text{st,s}}}, \quad (16)$$

and the equation for the current optimum rotational speed n_{opt} can be formed as a function of present H_{st} :

$$n_{\text{opt}}(H_{\text{st}}) = n_{\text{start}} + K \cdot H_{\text{st}}, \quad (17)$$

where n_{start} is the starting point of the speed profile. Any known static head value and its optimum rotational speed could be used to calculate n_{start} . In the simulations, n_{start} is replaced with $H_{\text{st,s}}$ related optimum rotational speed $n_{\text{opt,s}}$, and pump operation was eventually simulated as described above to determine the resulting energy consumption per emptied reservoir in each case.

Results

The resulting energy efficiency of both speed control schemes was studied through simulations for a Sulzer APP22-80 radial-flow centrifugal pump in a pumping process with a constant friction loss factor k of $0.0149 \times 10^{-6} \text{ s}^2/\text{m}^5$ and with various ranges of static head. Base value for the friction loss factor is based on the optimal pump dimensioning, when there is about 5 m of process static head. Also, the effect of friction loss factor on the results has been simulated, which will be discussed in the “Effect of surrounding process variables on the available saving potential” section.

Verification of the pump model operation

Correct operation of the chosen pump model (6) together with formed Eqs. (11) and (15) was first evaluated by operating the Sulzer pump at various rotational speeds in the Matlab simulation environment. Figure 2 illustrates the resulting characteristic curves for this pump with $Q_{\text{BEP},n} = 0.0276 \text{ m}^3/\text{s}$, $H_{\text{BEP},n} = 16.33 \text{ m}$, $H_{\text{max},n} = 21.87 \text{ m}$, $\eta_{\text{BEP},n} = 73\%$, and $n_n = 1450 \text{ rpm}$ as input parameters, when (6) and (13) are applied. Also, the effect of pump operation at 1200 and 950 rpm is illustrated with the help of (11) and (15) to show their effect on the pump models. To evaluate the correctness of (11) and (15), these two resulting curves have also been transformed with affinity laws (8)–(10) to two lower rotational speeds. As expected, QH characteristic curves obtained with (11) and affinity laws are identical to each

other. In $Q\eta$ curves, one can see the slight decreasing effect of rotational speed on the resulting curves when (15) is applied.

Available energy-saving potential with different control schemes

Simulation runs for different static head ranges were conducted as described in the “Simulation of studied control schemes” section. Energy consumption of drainage events per emptied reservoir with different values of static head variation ΔH_{st} and different levels of static head $H_{\text{st,e}}$ were calculated by conducting the simulation run. For each combination of static heads (i.e., for each kind of drainage event), the energy consumption was calculated for the studied speed control methods and for pump operation at the fixed (nominal) speed of 1450 rpm. Here, a drainage event includes all the time instances between the moments of $H_{\text{st,s}}$ and $H_{\text{st,e}}$ with 1-s time interval.

The simulated data has been combined into graphs that allow determination of the most suitable control scheme for the pumping process. The resulting graphs illustrate the energy-saving potential of the studied speed control methods in percent by comparing their specific energy consumption with that of fixed-speed operation at the nominal 1450 rpm:

$$\Delta E_s = \frac{E_{s,1450 \text{ rpm}} - E_{s,\text{nopt}}}{E_{s,1450 \text{ rpm}}} \cdot 100\%. \quad (18)$$

Since the pumped volume is identical in these comparisons between different control schemes, (18) can be directly used as the measure of energy-saving potential in percent.

Figure 3 illustrates the energy-saving potential, when the pumping system is operated at the best constant rotational speed instead of 1450 rpm. It appears that when the process static head decreases, the available energy saving potential increases, while ΔH_{st} has only a slight effect on the resulting energy-saving potential. It can also be seen that the best constant speed for drainage event is close to 1450 rpm when $H_{\text{st,e}}$ is around 75% of H_{max} , as the resulting energy saving potential is below 5%.

Figure 4 illustrates the energy-saving potential, when a linear rotational speed profile is applied instead of operating the pump at the fixed speed of 1450 rpm. Also

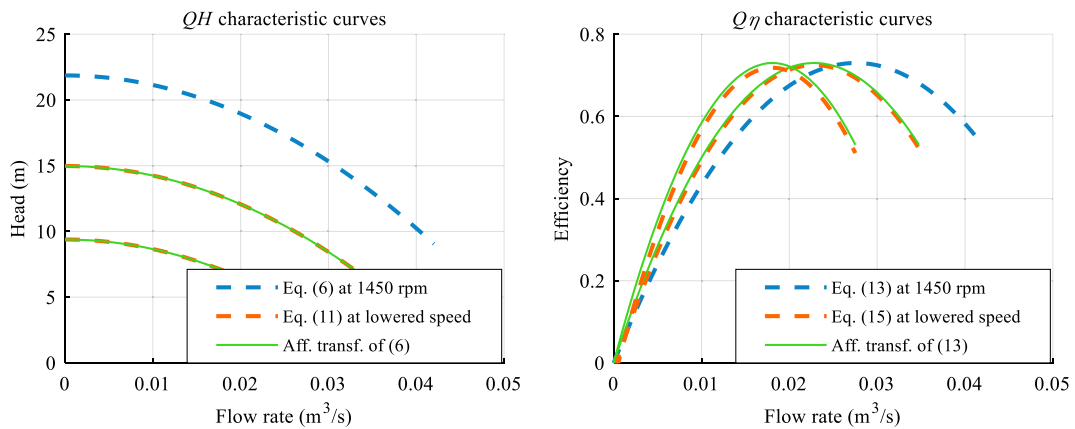


Fig. 2 The resulting characteristic curves for a radial-flow centrifugal pump at the nominal rotational speed of 1450 rpm and at the reduced speeds of 1200 and 950 rpm

here, a decrease in the process static head increases the available saving potential. Compared to Fig. 3, the amount of ΔH_{st} has a stronger effect on the resulting energy-saving potential, as ΔH_{st} can be compensated with the linear rotational speed profile.

Figure 5 illustrates the resulting difference in the energy-saving potential between these two control schemes. With a high level of ΔH_{st} , the linear speed profile can be more than 10% units more energy efficient than the pump operation at a certain constant rotational speed. This is expected, as the change in process static head directly affects the related E_s -based

optimum rotational speed as shown in Ahonen et al. (2015).

Effect of surrounding process variables on the available saving potential

When the same Sulzer pump is applied to a different pumping environment, the surrounding process variables, such as the static head and friction loss factor, will differ from their assumed values. Friction loss factor is affected by the length and diameter of piping together with characteristics of piping components, such as non-

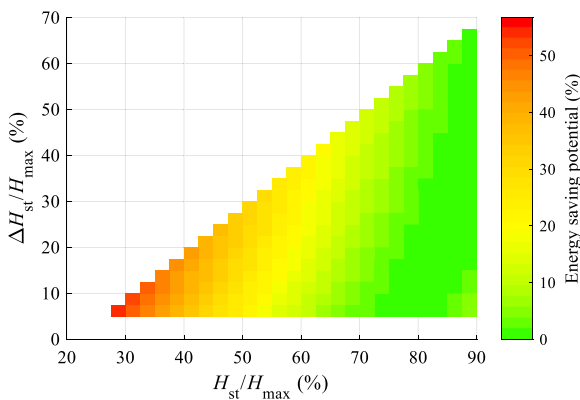


Fig. 3 The resulting energy saving potential in percent, when the exemplary pumping system is operated at a certain constant rotational speed and at various ranges of static head. Horizontal axis represents the share of process static head that directly affects the overall suitability of lowered speed operation. Vertical axis represents the change in process static head during the reservoir drainage, which affects suitability of operating the pump at a constant rotational speed

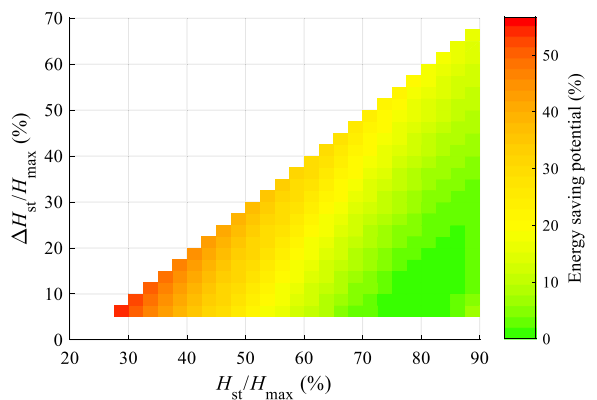


Fig. 4 The resulting energy-saving potential in percent, when the exemplary pumping system is operated with linear rotational speed profiles and at various ranges of static head. Horizontal axis represents the share of process static head that directly affects the overall suitability of lowered speed operation. Vertical axis represents the change in process static head during the reservoir drainage, which favors the use of linear rotational speed profiles

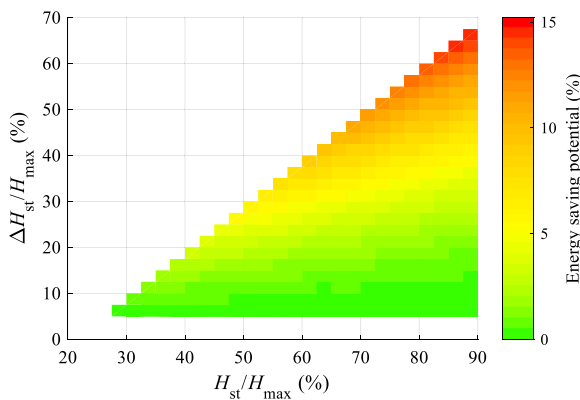


Fig. 5 Difference in the available energy-saving potential between the two VSD-based control methods are given in percent units. The advantage of the linear speed profile control over the pump operation at a certain constant rotational speed becomes more significant when variation in the process static head increases

return valves and piping bends, meaning that the absolute value of k will be unique to each pumping environment. To assess the effect of the friction loss factor on these two control schemes, the pumping process was simulated by using different values for the friction loss factor.

Figure 6 illustrates the resulting curves with the green line representing the base amount of k ($0.0149 \times 10^{-6} \text{ s}^2/\text{m}^5$). The orange line corresponds to an environment with doubled amount of friction losses and the blue line to an environment with halved friction losses compared to the base amount. It appears that while the amount of friction losses in the system does contribute to the amount of available energy-saving potential, it is not significant enough to change the illustrated basic behavior of available saving potential, and hence, the resulting basic shape of the above-presented graphs. This indicates that the graphs in Figs. 3, 4, and 5 should be feasible for reservoir pumping systems with a variety of friction losses, if the same pump for which the graphs were generated is in the setup.

Evaluation of pilot cases

To see if the graphs introduced above provide correct information, the calculus was applied to two real-life cases with known characteristics. Both of these cases have been previously evaluated to determine their available energy-saving potential through the variable-speed operation in Ahonen et al. (2015). The findings of these

studies are used to validate the results given by graphs in Figs. 3 and 4.

The first case is called Pietarsaari. It is a wastewater pumping station, which is a fine example of a centrifugal pumping process. A study for this case was done by estimating the amount of energy-saving potential with Figs. 3 and 4, when the process static head rises from 2 to 5 m, and the pump maximum head is 18 m (i.e., $\Delta H_{st}/H_{max} = 17\%$; $H_{st,e}/H_{max} = 28\%$). Figure 7 illustrates the original pump QH characteristic curve in the Pietarsaari case, the QH curve provided by (6) and the surrounding system with maximum process static head. A significant difference can be seen in the shapes of the actual and estimated pump QH characteristic curves, which may affect the estimation results for this case.

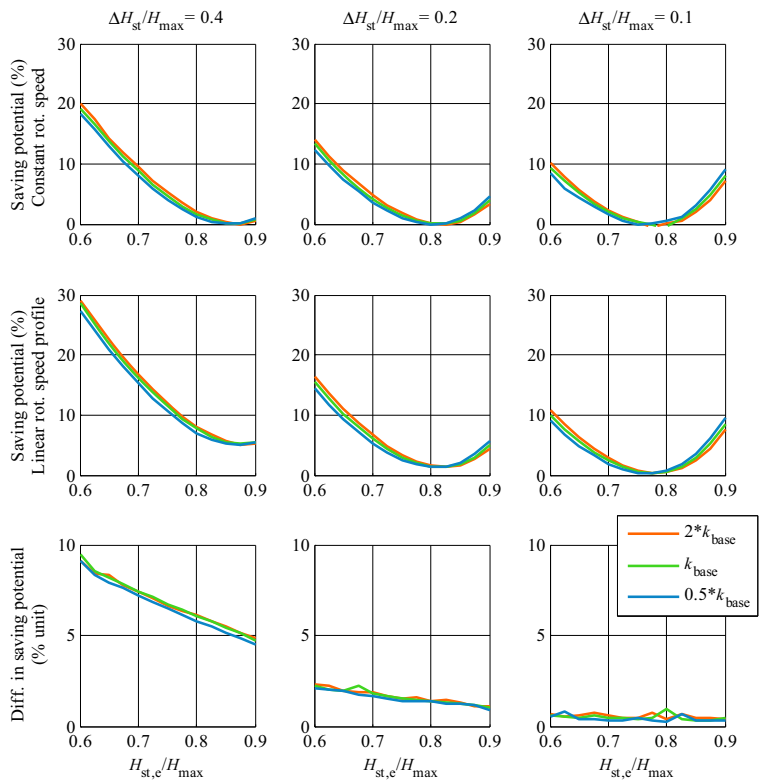
Based on Fig. 3, the estimated energy-saving potential with the best constant rotational speed operation is about 43%. With the linear speed profile, this value increases to 47%. In Ruuskanen (2007), the amount of available energy-saving potential at the best constant speed was calculated to be around 40–45%, being very close to the result provided by Fig. 3.

Since the amount of static head variation during the pumping task is low, additional energy-saving potential through the use of linear speed profile cannot be significant. In this case, the relative amount of static head variation was 17%, resulting in additional energy-saving potential between 2 and 4% units according to Fig. 5, which is in the error margin of previously calculated energy saving potential.

The second case is called Heimosilta. It is also a wastewater pumping station with system characteristics as illustrated in Fig. 8. Since the pump QH characteristic curve is only known for a limited flow rate range, H_{max} was approximated to be 35.5 m, leading to $\Delta H_{st}/H_{max} = 2\%$; $H_{st,e}/H_{max} = 36\%$. This station was selected for the analysis, because it has a very small variation in the static head (ca. 1 m) and very low friction losses ($k = 0.00048 \times 10^{-6} \text{ s}^2/\text{m}^5$, about 3% of k_{base}) compared to the reference case.

A separate field study has been conducted on this station to test if the flow control method could be optimized better. Test runs were conducted at different constant rotational speeds for the study with 18% energy-saving potential as a main result compared with the pump operation at its nominal rotational speed. Based on Figs. 3 and 4, the available saving potential should be around 36%, which clearly differs from the measured values. This is mainly caused by the

Fig. 6 Comparison between the available energy-saving potential with two different control schemes and different amounts of static head variation and friction losses. Higher variation in static head results in a larger difference in the energy saving potential between the two control methods. Change in friction loss factor results in just a slight difference into the graphs, indicating the feasibility of Figs. 3, 4, and 5 for different systems



difference in friction loss factors between the reference system and this case. This has been ensured by calculating separate energy-saving potential graphs for the Heimosilta case with 18% as a result for the available energy-saving potential both with the constant speed operation and with linear rotational speed profile.

With these two limited example cases, it can be noted that the graphs in Figs. 3, 4, and 5 yield indicative results with reasonable accuracy even for pumps with notably different QH characteristic curve shape. It can be expected that the results and their accuracy will vary when the actual pump curve and

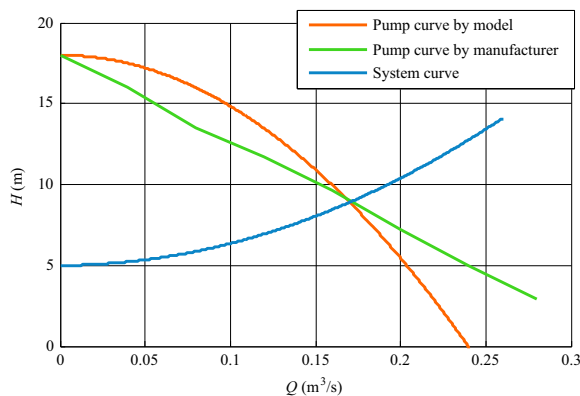


Fig. 7 Pump curves and system curve for case Pietarsaari. Equation (6) does not represent identically the actual shape of the pump QH characteristic curve. In spite of this, energy-saving potential with the variable-speed operation can be correctly determined with Figs. 3 and 4

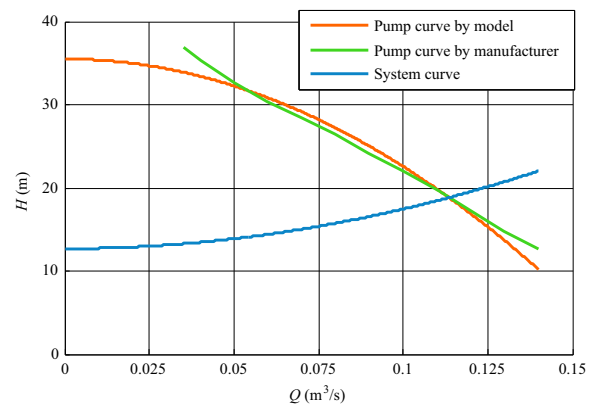


Fig. 8 Pump curves and system curve for case Heimosilta. Neither here does (6) represent identically the actual shape of the pump QH characteristic curve. In addition, k representing the system curve shape is only 3% of k_{base}

surrounding system characteristics differ more from the base setup introduced in the “Results” section. If accurate results are sought after instead of utilizing Figs. 3, 4, and 5, they can be solved by applying the simulation as described in the “Simulation of studied control schemes” section for the pump and system in question.

Conclusion

Reservoir pumping applications are often equipped with fixed-speed pumps that may also be oversized for common process requirements. Retrofitting the pumping system with VSD-based speed control can provide considerable energy and cost savings. Determining the available benefits of the variable-speed operation normally requires insight on the pumping process and technical characteristics of existing pumps. However, some parameters of the process can be more easily determined, such as the amount of static head and its variation during the drainage, since these are general characteristics of the reservoir pumping system. Characteristics of the pump may also be easily available, if they are provided by manufacturer.

Unless the pumping process is especially tailored to use a single constant rotational speed and it happens to be the nominal rotational speed of the pump, energy will be wasted. The potential energy savings can be as high as 40% when retrofitting a VSD into a constant speed pumping system.

In this study, two VSD-based speed control methods were introduced and simulated with a centrifugal pump to create a graphic analysis tool, which could be used for the quick estimation of available energy-saving potential using that specific pump in a different pumping environment.

The produced graphs for available energy-saving potential seem to provide credible results when compared to the results of two case studies, which justifies their use for instance in energy auditing. However, further testing would be required to see whether the resulted graphs represent reality in all situations that arise from static head and its variation. Also, even though the friction loss factor was not as impactful variable as the static head was, it can vary much more than what was simulated in this study and skew the gained results. Overall, if there is a demand for flow control in the process, installing a variable-speed drive to a new system or retrofitting it to an older one instead

of running the pump at its nominal speed has been calculated to provide a significant reduction in the system energy consumption.

Funding information This work was carried out in the Efficient Energy Use (EFEU) research program coordinated by CLIC Innovation Ltd. with funding from the Finnish Funding Agency for Technology and Innovation, Tekes. Research work has also been funded by Academy of Finland.

Compliance with ethical standards

Conflict of interest The authors declare that they have no conflict of interest.

References

- Ahonen, T., Tamminen, J., Viholainen, J., Ahola, J., & Koponen, J. (2015). Energy efficiency optimizing speed control method for reservoir pumping applications. *Energy Efficiency*, 8(1), 117–128.
- Barnes S. (2014). Energy efficient variable frequency drives and submersible pumps. Proceedings of Australia’s international water conference and exhibition (Ozwater’14). Brisbane, Australia.
- Bene J. (2013). Pump schedule optimization techniques for water distribution systems. Oulu.
- de Almeida, A. T., Fonseca, P., & Bertoldi, P. (2003). Energy-efficient motor systems in the industrial and in the services sectors in the European Union: characterisation, potentials, barriers and policies. *Energy*, 28(7), 673–690.
- dos Santos, J. N., & Selegheim Jr., P. (2005). Optimized strategies for fluid transport and reservoirs management. *Revista Minerva-Pesquisa & Tecnologia*, 2(1), 91–98.
- Flygt (2015). Variable speed wastewater pumping, white paper.
- Gulich, J. F. (2003). Effect of Reynolds number and surface roughness on the efficiency of centrifugal pumps. *Journal of Fluids Engineering*, 125(4), 670–679.
- Hovstadius, G. (1999). Economical aspects of adjustable speed drives in pumping systems. Proceedings of 21st National Industrial Energy Technology Conference. May 12–13. 1999. Houston, Texas, USA.
- Hovstadius G. (2005). Getting it right, applying a systems approach to variable speed pumping. Proceedings of 4th international conference on energy efficiency in motor driven systems (EEMODS ‘05), Heidelberg, Germany.
- Kallesøe C. S. (2005). Fault detection and isolation in centrifugal pumps. Aalborg.
- Kallesøe, C. S., Skødt, J., & Eriksen, M. (2011). Optimal control in sewage applications. *World Pumps*, 2011, 20–23.
- Kaya, D., Yagmur, E. A., Yigit, K. S., Kilic, F. C., Eren, A. S., & Celik, C. (2008). Energy efficiency in pumps. *Energy Conversion and Management*, 49(6), 1662–1673.
- Lindstedt M. & Karvinen R. (2015). Optimal speed control of two unequal parallel pumps in reservoir filling: minimum energy

- with fixed time. Proceedings of ECOS 2015—28th international conference on efficiency, cost, Simulation and environmental impact of energy systems. Pau, France.
- Lindstedt, M., & Karvinen, R. (2016). Optimal control of pump rotational speed in filling and emptying a reservoir: minimum energy consumption with fixed time. *Energy Efficiency*, 9(6), 1461–1474.
- Middleton, P. (2014). SmartRun, VSDs and optimised wastewater pumping. *Mechanical Technology*, 34–37.
- Nesbitt B. (2006). Handbook of pumps and pumping: Pumping manual international.
- Pump Systems Matter & Hydraulic Institute (2008). Optimizing pumping systems guidebook.
- Ruuskanen A. (2007). Optimization of energy consumption in wastewater pumping. Helsinki.
- Sârbu, I., & Borza, I. (1998). Energetic optimization of water pumping in distribution systems. *Periodica Polytechnica Ser. Mech. Eng.*, 42(2), 141–152.
- Schützhold J., Benath K., Müller V. & Hofmann W. (2013). Design criteria for energy efficient pump drive systems. Proceedings of EPE'13 ECCE Europe Conference. Lille, France.
- Shankar, A., Kalaiselvan, V., Umashankar, S., Paramasivam, S., & Haginovszki, R. (2016). A comprehensive review on energy efficiency enhancement initiatives in centrifugal pumping system. *Applied Energy*, 181, 491–513.
- Tamminen J., Viholainen J., Ahonen T. & Tolvanen J. (2013). Sensorless specific energy optimization of a variable-speed-driven pumping system. Proceedings of 8th international conference on energy efficiency in motor driven systems (EEMODS'13). Rio de Janeiro, Brazil.
- Xylem. (2013). Intelligent control for flow variations. *World Pumps*, 2013(5), 22–23.
- Zhang, H., Xia, X., & Zhang, J. (2012). Optimal sizing and operation of pumping systems to achieve energy efficiency and load shifting. *Electric Power Systems Research*, 86(5), 41–50.